Reliability-based safety factor for metallic strip flexible pipe subjected to external pressure

Ting Liu[a,*], Bernt J. Leira[b], Ping Fu[b], Yong Bai[a], Dahui Liu[a,c]

[a] College of Civil Engineering and Architecture, Zhejiang University, Hangzhou, PR China
[b] Department of Marine Technology, Norwegian University of Science and Technology, NO-7491 Trondheim, Norway
[c]CIMC Offshore Engineering Institute Co., Ltd, Yantai, PR China

Abstract: Reliability-based safety factors for metallic strip flexible pipes(MSFP) subjected to external pressure are calibrated in this paper. The partial safety factors of such pipes are obtained by introducing a target reliability index and using a combination of Monte-Carlo simulation and FORM. The relationship between the safety factors and the coefficient of variation for key basic variables as well as the impact of different distribution types for both the resistance and load effect parameters on the calibrated results are investigated. Recommended design safety factor for MSFP is given similar to the widely used design safety factor for conventional metallic pipes. The calibration process presented in this paper is relatively easy to understand and to carry out. This also applies to cases with multiple components and even requiring complex iterations in relation to the mechanical model. The results obtained here can provide some guidance in connection with manufacturing procedures at the initial design stage of the MSFP.

Keywords: Metallic strip flexible pipe, reliability analysis, Monte-Carlo simulation, FORM, partial safety factors.

1. Introduction

Metallic strip flexible pipes (MSFP) represent a novel category of composite pipes. Similar to classic flexible pipes, they are composed of an inner PE layer, an outer PE sheath, and helical metallic layers. The difference from other flexible pipes is that the metallic layers in MSFP are of a simple type. They do not contain the complicated interlocked carcass layer, the pressure armour layer, and the tension armor layers, which are the essential constituents in flexible pipelines (API-RP-17B, 2008). Instead, the MSFP only consist of helically wound steel strips. This simplified configuration makes MSFP much more cost effective due to the convenient manufacturing process. Its typical cross section and manufacturing process are shown in Fig.1. Compared with the widely applied reinforced thermoplastic pipes (RTP), MSFP do not only possess the good properties of RTP, but they can also contribute a lot to improve on-bottom stability properties because of their relatively heavier weight. Therefore, for shallow water applications, where the operating requirements are not so demanding, MSFP may represent a first choice of pipe concept. Although MSFP are designed primarily for shallow water applications, its collapse capacity with respect to external overpressure is still a great challenge due to the lack of a carcass layer. During operation, MSFP might face a number of uncertainties that also represent a challenge. This implies that application of design safety factors which are adequate in order to ensure a sufficient reliability level is of key importance. Hence, the reliability level of MSFP when subjected to external pressure needs to be quantified and kept at a high enough level. Appropriate design safety factors should be prescribed in order to reach this target safety level, but also in order to avoid unnecessary conservatism.
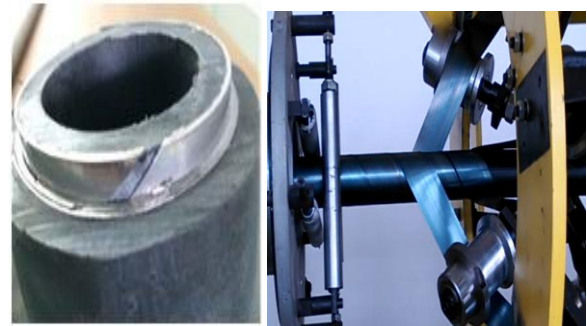

Fig.1. Cross section and manufacturing process of MSFP.

During the last decades, comprehend amount of research has been performed within the area of pipeline reliability analysis. Babu, et al. (2010) addressed the reliability associated with buried flexible pipe-soil systems. Tee, et al (2013) investigated the reliability level associated with underground flexible pipes. Extensive analyses relating to reliability of pipelines with corrosion defects can also be found in the existing literature (Ahammed, et al., 1996; Teixeira, et al., 2008; Leira, et al., 2016; Larin, et al., 2016). As for reliability-based safety factors to be applied for pipeline design, Boyer, et al. (1997) undertook the calibration of design safety factors for a composite pipe in order to illustrate the different steps of the procedure. Leira, et al. (2005a, 2005b) proposed a structural reliability-based approach for fatigue analysis of flexible pipes and established the relationship between the fatigue safety factors and the inherent failure probability. Based on the above method, dos Santos, et al. (2012) performed a calibration of safety factors to be applied for fatigue analysis of flexible riser tension armours. Avrithi and Ayyub (2010) described the development of design equations according to the load and resistance factor design (LRFD) method for loads that cause primary stress for different levels of piping operation and illustrated the

partial safety factors for different values of the target reliability index. In the same year, Machida, et al. (2010) illustrated the evaluation of partial safety factors for parameters related to flaw evaluation of pipes, and proposed the important matter which should be paid attention to in the setup of the safety factors used in flaw evaluation. Fairchild, et al. (2016) described the use of the previous full-scale tests data to develop a safety factor for strain-based engineering critical assessment of pipelines. Likewise, in combination with experimental data, Schillo, et al. (2017) suggested a reliability based calibration method of safety factors for the unstiffened composite cylinder shell relying on extensive measurements regarding the statistical characteristics of the geometrical and material properties of 11 previously tested composite cylinders.

As MSFP is a relatively new type of pipe concept, its mechanical behavior is still not fully understood, not to mention the inherent reliability level during operation. According to the best knowledge of the authors, there are hardly any publications dealing with calibration of safety factors for MSFP. As the collapse pressure is of primary concern for the ultimate capacity of pipelines in operation, the safety factors associated with design to withstand external pressure are calibrated in the present paper.

A simplified mathematical model for calculating the collapse pressure of MSFP can be obtained from recent work performed by Bai, et al. (2016a). For the classic analytical model associated with elastic buckling of a ring or a cylinder, the calculation is straightforward. However, the plastic behavior of the PE material has a significant impact on the collapse pressure. The nonlinearity of the PE material which is taken into account in Bai's (2016a) capacity model improves the accuracy of the results, but also introduces some challenges in relation to the reliability-based safety factor analysis. The purpose of this paper is to propose a calibration process for MSFP by using a combination of Monte-Carlo simulation and FORM. The method was referenced and extended from the reliability analysis of RTP in Ref. (Bai, et al., 2017). Sensitivity analyses are conducted with respect to the key parameters which influence the values of the safety factors. The design safety factor for MSFP is recommended at the end of the paper. The factor is to be seen in light of the design safety factor of 1.5 (Zhu, 1993) which is widely applied for conventional pure metallic structures(pipes).

2. Calibration process for safety factors

Uncertainties are always involved when conducting strength evaluation and structural analysis. Before starting the calibration, the basic variables corresponding to the design parameters should be determined, and the uncertainties related to the prediction of resistance and load effect should be taken into account.

As the MSFP is composed of many layers, the basic variables are too many to calculate the associated probability exactly when using full integration or general reliability methods. The accuracy and feasibility of the well-known first and second order reliability method

(FORM/SORM) in estimating the results can be rather dubious in the present case. In addition, an iterative method is required in order to calculate the resistance of the MSFP. This makes it very demanding to apply FORM/SORM techniques directly. Here, the Monte-Carlo method can be regarded as a good approach in order to estimate the statistical properties of the resistance term. First, groups of random sample values of the basic variables related to the resistance of the MSFP can be generated according to their respectively stochastic models. By introducing all those generated variables and uncertainty factors into the resistance model, a corresponding array of the collapse pressure can be obtained. Through the statistical analysis, the distribution type and the corresponding parameters of the resistance term can be obtained. With the statistical models of the resistance and load random variables R and S being known, it is easy to calculate the failure probability P_f and the corresponding reliability index β :

$$p_f = prob(R < S) \tag{1}$$

$$\beta \approx \Phi^{-1}(-P_f) \tag{2}$$

where, $\Phi^{-1}(\bullet)$ is the inverse of the standard normal distribution function. As the limit state function has a simple form with statistical models established through the above simulation steps, the well-known methods mentioned above can now be used to calculated the reliability, such as FORM, SORM, Importance sampling, etc. Among these methods, FORM is particularly popular as it is easy to understand and efficient to apply. Furthermore, it can provide relatively accurate result. The reliability index in FORM is obtained by calculating the shortest distance from the origin point to the limit state surface in the standard normal space, and the corresponding point in the limit state surface is referred to as the design point. This point is also crucial in order to calculate the partial safety factors. The partial safety factors used in the load and resistance partial safety factor design (LRFD) equation are expressed as:

$$R / \gamma_R \geq \gamma_S \cdot S \tag{3}$$

where, γ_R and γ_S are the partial safety factors for resistance and load, respectively. In order to reach the given target reliability index $\beta_{t\,arg}$, the mean value of the resistance force μ_R can be adjusted while both R's coefficient of variation δ_R and S's distribution parameters μ_S, δ_S are kept unchanged. After reaching the target reliability level, the final coordinates of the design point are obtained, i.e. R^* and S^*. The partial safety factors can then be calculated through the following equations:

$$\gamma_R = R_K / R^* \tag{4}$$

$$\gamma_S = S^* / S_K \tag{5}$$

where, R_K and S_K are the specified characteristic values of the resistance and load effect, respectively. The subscript K represents the given probability of exceedance that is aimed at. The characteristic value can be obtained from the particular fractiles of the relevant density

functions. Usually upper and lower fractiles are applied. In this paper, a lower fractile for the resistance where K equals 0.025 is employed, while for the load effect, an upper fractile that K equals 0.975 is selected in order to ensure a safe design. It should also be mentioned that the characteristic value R_K changes with the adjustment of μ_R during the calibration process. By multiplying the two partial safety factors, the "design safety factor" k can then be obtained as follows:

$$k = \gamma_R \gamma_S \qquad (6)$$

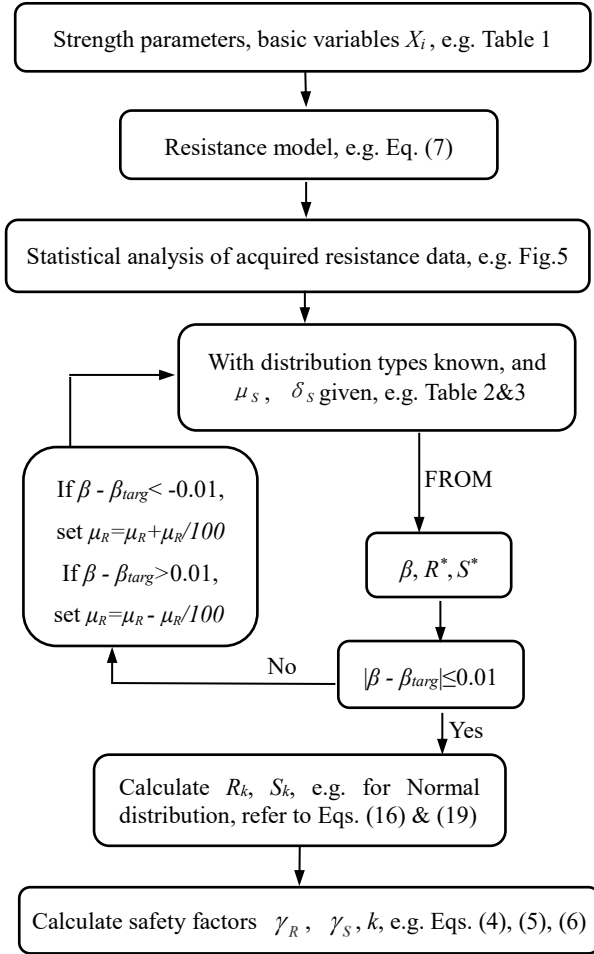A flow-chart which represents the calculation process for the safety factors is illustrated in Fig.2.

```
┌─────────────────────────────────────────────────┐
│ Strength parameters, basic variables Xᵢ, e.g. Table 1 │
└─────────────────────────────────────────────────┘
                      ↓
┌─────────────────────────────────────────────────┐
│         Resistance model, e.g. Eq. (7)          │
└─────────────────────────────────────────────────┘
                      ↓
┌─────────────────────────────────────────────────┐
│ Statistical analysis of acquired resistance data, e.g. Fig.5 │
└─────────────────────────────────────────────────┘
                      ↓
┌─────────────────────────────────────────────────┐
│     With distribution types known, and          │
│      μ_S , δ_S given, e.g. Table 2&3             │
└─────────────────────────────────────────────────┘
```

If β - β_{targ}< -0.01, set μ_R=μ_R+μ_R/100
If β - β_{targ}>0.01, set μ_R=μ_R - μ_R/100

FROM

β, R^*, S^*

No

$|\beta$ - $\beta_{targ}|\leq$0.01

Yes

Calculate R_k, S_k, e.g. for Normal distribution, refer to Eqs. (16) & (19)

Calculate safety factors γ_R, γ_S, k, e.g. Eqs. (4), (5), (6)

Fig.2. Flowchart for the calculation process.

3. Calibration for MSFP under external pressure

3.1. Mechanical model

The collapse pressure of MSFP when subjected to external pressure can be obtained from the formula given by Bai, et al. (2016a) as:

$$P_{cr} = \sum_{i=1}^{N_i} P_{cr,\text{steel}}^i + \sum_{j=1}^{N_j} P_{cr,PE}^j \qquad (7)$$

where, i and j are the layer number for steel reinforcement layers and PE tubes; N_i and N_j are their

respective number of layers. As it is reasonable to regard the steel strips as pure elastic in the buckling analysis (Bai, et al., 2016a), the contribution from the steel strip layers can be expressed as:

$$P_{cr,steel}^i = \varphi n E_{ste,i} bh^3 / 4L_p R_i^3 \qquad (8)$$

where, n is the number of strips in the layer; L_p is the pitch; $E_{ste,i}$ is the elastic modulus of the steel material; b and h are the width and thickness of the steel strip; φ is a factor that depends on the lay angle and the moment of inertia for the section; R_i is the mean radius of the ith layer. For the PE layers, the tangent modulus method can be applied in order to calculate their contributions:

$$P_{cr,PE}^j = \frac{3E_{j,t}^f I_j^f}{R_{j,f}^3} \qquad (9)$$

where, the superscript f refers to the fth increment step; $E_{j,t}$ is the tangent modulus of the jth layer; I_j is the equivalent moment of inertia and R_j is the updated mean radius of the tube.

The method for calculation of the PE tube's capacity is illustrated in detail in Ref. (Bai, et al., 2015). The general idea can be summarized as follows: The assumed radial deformation is applied to the outside surface of the tube step by step. When the deformation is given at each step, the radial strain of the tube can be calculated, and the radial stress can then be obtained from the given stress-strain relationship of the PE material. The tangent modulus, the current layer thickness and its mean radius can then be updated. The compressive pressure (i.e. the assumed external pressure) is obtained by accumulating the stress in the radial direction. By substituting the updated tangent modulus and physical dimensions at each step into Eq. (9), the plastic buckling pressure under the assumed deformation is calculated. If the calculated plastic buckling pressure corresponding to the assumed deformation is equal to the compressive pressure, this pressure is registered as the ultimate strength for the tube. A diagram which illustrates the calculation process is shown in Fig.3.
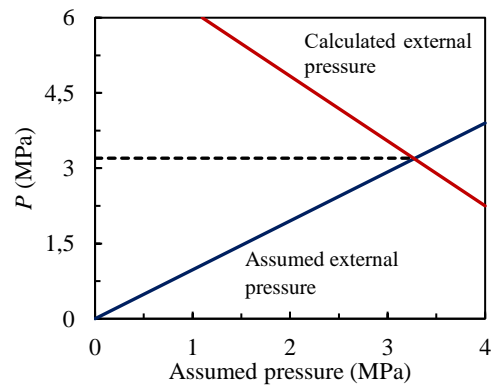

Fig. 3. Determination of plastic buckling pressure for the PE layers (Bai, et al., 2015).

By summing the contributions from all the separate layers, the collapse pressure of the MSFP is obtained. The pipe's performance function G on bearing the collapse pressure can be written as:

$$G = R - S \qquad (10)$$

where, R represents the resistance capacity of the pipe P_{cr}, and S refers to the external pressure that the pipe is subjected to.

3.2. Stochastic model

The stochastic models for basic random variables associated with the resistance term are shown in Table 1. The structure and geometry of the MSFP studied in the present paper are the same as those in Ref. (Bai, et al., 2016a). The distribution types of the geometrical and material properties of the pipe are determined according to the recommendations of DNV (1992). The subscript i and o of R in Table 1 represents inner and outer radius values, respectively. The first subscript represents the PE layer's location while the second one represents the reference diameter. For instance, R_{ii} indicates the inner radius of the inner PE tube, while R_{io} is the outer radius of the inner PE tube. α is the winding angle of the steel strips and μ_{PE} is the Poisson's ratio of the PE material.

Table 1. Probability models for resistance basic variables

Variable	Unit	Mean value	CoV	Prob.dist.
R_{ii}	mm	25	0.01	N
R_{io}	mm	31	0.01	N
R_{oi}	mm	33	0.02	N
R_{oo}	mm	37	0.02	N
b	mm	52	0.01	N
h	mm	0.5	0.01	N
α	°	54.7	0.03	N
E_{ste}	GPa	199	0.06	N
μ_{PE}	-	0.4	0.06	N

Note: CoV means coefficient of variation; N in the last column refers to the Normal distribution.

In order to take the PE material's plasticity and parameter uncertainty into account, its properties can be modeled with nonlinear material parameters. The stress–strain relationship can be expressed as follows (Gibson, et al., 2000):

$$\sigma = \frac{E_0}{\kappa}(1 - e^{-\kappa \varepsilon}) \qquad (11)$$

where σ and ε are the stress and strain; κ is a constant which can be determined from a given experimental curve. The tangent modulus derived from Eq. (11) can be expressed as:

$$E_t = E_0 e^{-\kappa \varepsilon} \qquad (12)$$

The stress-strain curve of the PE material is in accordance with the one given in Ref. (Bai, et al., 2016a). The experimental data and the fitted curve are shown in Fig.4. The parameter κ in Eq. (11) determines the trend of the curve. For simplicity, the PE material's uncertainty can be modeled by regarding κ as a normally distributed variable. The mean value of κ is set to be 46 from the fitted curve and its coefficient of variation (CoV) is selected as 0.05 which can give a reasonable variation range for the resulting material curves.
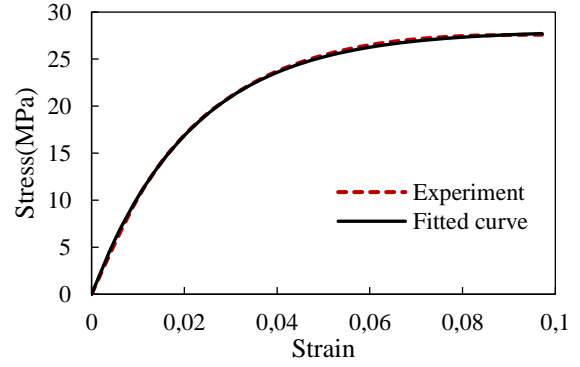

Fig.4. Stress-strain curves for the PE material.

The collapse pressure calculated based on Eq. (7) is usually used as a lower limit value for the MSFP. The initial ovality of the pipe is not taken into account in this mechanical model, but contributes significantly to the model uncertainty. The distribution parameters of the model uncertainty can hence be selected according to the effect of the uncertainty associated with the initial ovality of the pipe. Based on the limited amount of measured data for the initial ovality of the MSFP in Ref. (Bai, et al., 2016b), its schematic density function can be drawn with a mean value which is found to be around 0.5%. Through comparison between variation of FEM calculation results, experiments and the ovality model, the mean value for the model uncertainty variable is selected as 1.05, and its corresponding CoV is chosen as 0.1. Its distribution function is still represented by a Normal model.

By using Monte Carlo simulation and substituting all the sample values of the basic variables into the mechanical model of the resistance, a series of random sample values for collapse pressure is obtained. The probability distribution function (PDF) of the resistance pressure can be acquired by using curve fitting as shown in Fig.5. The statistical properties of the resistance variable obtained from the above stochastic models are listed in Table 2.
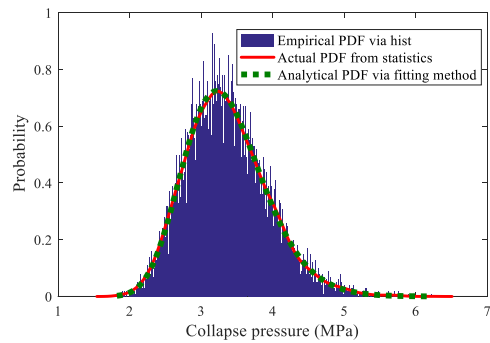

Fig.5. Histogram and probability distribution of MSFP's resistance pressure.

Table 2. Statistical properties of resistance pressure for the MSFP

Mean value	Stand.dev.	CoV	Prob.dist.
3.3576MPa	0.5656	0.1685	Normal

According to Ref. (DNV, 1992), a Log-normal distribution can be used for the load variable. The mean value can be

determined based on the relevant water depth which is about 100 meters in the present study. The distribution parameters for the load effect are shown in Table 3.

Table 3. Statistical properties of load effect

Mean value	Stand.dev.	CoV	Prob.dist.
1MPa	0.1	0.1	Log-normal

3.3. Analysis and discussion of the results

The safety factors are closely related to the target reliablity index $\beta_{\text{t arg}}$, and their relationships are shown in Fig.6. From this graph, it can be seen that, γ_R increases with the increase of $\beta_{\text{t arg}}$ while the value of γ_S is almost unchanged. This is due to the fact that when increasing the target reliability, the mean value of the random variable R has to increase as well as its corresponding characteristic value. However, the design value calculated in this process does not change that much, resulting in an obvious increase of γ_R. It can also be noticed that, the increasing trend of k and γ_R in this case exhibit a parabolic apperance, and the growth rate is particularly high when $\beta_{\text{t arg}}$ is large. Generally speaking, the larger $\beta_{\text{t arg}}$ is, the greater the "design safety factor" k (see Fig.6) will be, which implies a smaller value of the failure probablity for the pipe. The relationship between the design safety factor k and the reliability of the pipe (which is defined as 1.0 minus the failure probability) is shown in Fig.7.
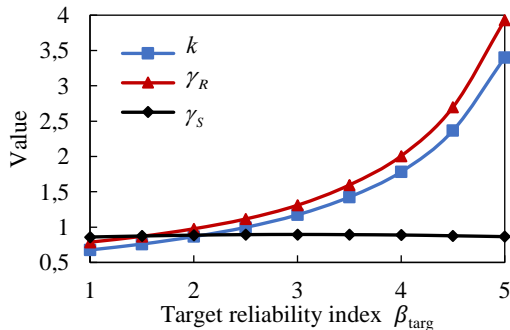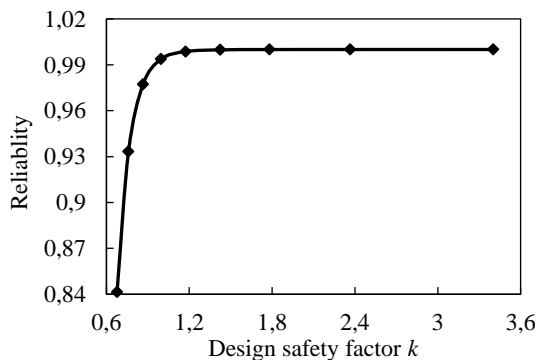

Fig.6. Safety factors vs target reliablity index.

Fig.7. Design safety factor k vs reliability (i.e. 1.0 minus the failure probability) of the MSFP.

As the innermost PE layer gives the highest contribution to the collapse pressure in present pipe, the effect of the variation of its inner radius on the design safety factor is investigated further. Although the initial ovality of the MSFP does not play that a significant role with respect to the ultimate strength as it does for pure metallic pipes, it still has a relatively dominating effect (as compared to other factors). Thus, the effect of changing the CoV of the two above-mentioned basic variables are investigated. When a target reliability index is given, the design safety factor k would most likely increase with the CoVs of the basic variables related to the resistance term. In this part, $\beta_{\text{t arg}}$ is selected as 4.0 to study the effect. The actual coefficient of variation for the ultimate strength of the MSFP would need to be controlled during the manufacturing process itself. Therefore, the analysis is mainly focused on the CoV of the resistance (i.e. δ_R), where values below 0.25 are considered, as the occurrence of a δ_R higher than 0.25 is hardly possible in reality. The relationship between δ_R and the CoVs for the model uncertainty (i.e. δ_{mod}) and for the inner radius (i.e. δ_{ii}) are shown in Fig.8.
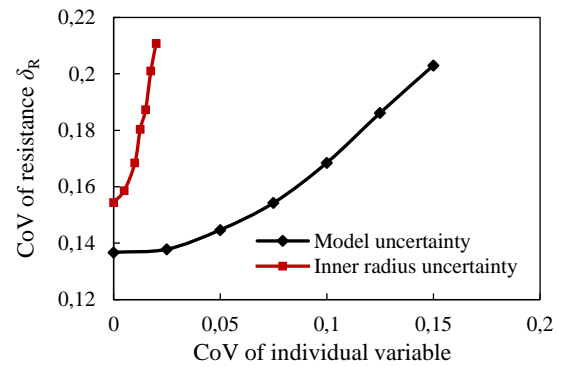

Fig.8. Effect of CoV representing uncertainties (related to model and inner radius) with respect to value of δ_R.

From Fig.8, it is seen that the inner radius uncertainty has the highest influence on δ_R. Variation of the inner radius does not only have an effect on the mean radius of the inner tube, but also on its thickness, which are the two key aspects that determine the collapse capacity of the tube. The relationship between the design safety factor k and the CoV for both the model uncertainty and the inner radius are shown in Fig.9(a) and Fig.9(b). Not unexpectedly, the design safety factor k increases with the increase of δ_{mod} and δ_{ii}, and the curve shows an exponential format. If k is kept as constant while the CoV of the related uncertainty increases, the changing trend of the reliability index β can also be helpful in estimating the effect. It can be seen from Fig.9(a) and Fig.9(b) that with a constant k value, β decreases with the increase of δ_{mod} & δ_{ii}.
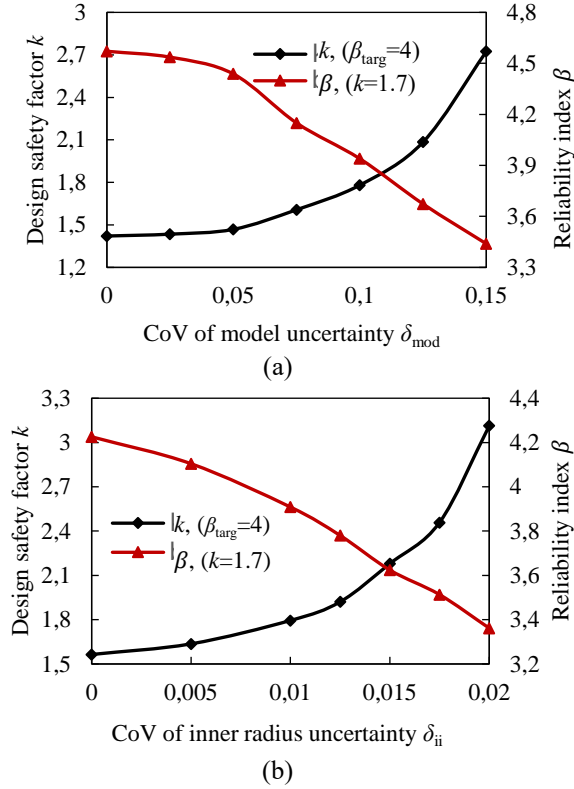
(a)

(b)

Fig.9. Design safety factor k and the reliability index β vs CoV of uncertainty related to: (a) δ_{mod} (b) δ_{ii}.

It is of interest to study the combined effect of those two factors δ_{mod} and δ_{ii}, so the variation of k with different joint CoVs for both the two variables is illustrated in Fig.10. As shown in the mesh plot, the design safety factor k increases with δ_{mod} and δ_{ii}. Taking a close look on the graph, it is observed that an interesting phenomenon occurs: the design safety factor k almost pops up abruptly for the highest values of the coefficients of variation. This further shows that when δ_{mod} and δ_{ii} are both relatively large, the increasing speed of the design safety factor k grows dramatically, every subsequent small increment for either δ_{mod} or δ_{ii} will result in several times enlargement of k. Meanwhile, the design safety factor k is closely related to the production cost of the pipe. In order to lower costs, the coefficient of variation for the uncertainties, especially for the inner radius uncertainty of the pipe should be controlled strictly during the manufacturing process.
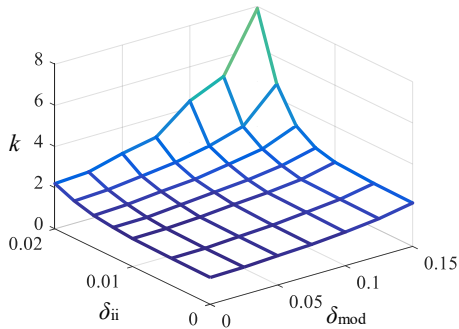

Fig.10. Design safety factor k vs δ_{mod} and δ_{ii}.

4. Effects of different distribution types

As the distribution types of the resistance and load effect might also have some impact on the calculated results, the three mostly applied distribution types are selected in order to study this sensitivity. The subtitles of the distribution types in this part are abbreviated, where N represents the Normal distribution while LN represents the Log-normal model. The first abbreviation in the subtitles refers to the resistance distribution while the second one refers to the load effect distribution.

4.1. N-N distributions

When the normally distributed parameters for resistance and load effect are known, it is easy to calculated the reliablity index:

$$\beta = (\mu_R - \mu_S) / \sqrt{(\mu_R \delta_R)^2 + (\mu_S \delta_S)^2} \qquad (13)$$

With the target reliablity index β_{targ} given, which can be regarded as a known quantity in Eq. (13), μ_R can be solved out from this quadratic equation. However, there are two roots of this equation, and the selection of the value should be paid special attention. Generally, μ_R should be larger than that of μ_S. In our case, the mean value for the resistance is selected as:

$$\mu_R = \mu_S[\sqrt{1 - (\beta_{targ}^2 \delta_R^2 - 1)(\beta_{targ}^2 \delta_S^2 - 1)} + 1] / (1 - \beta_{targ}^2 \delta_R^2) \qquad (14)$$

The design point of the resistance can be calculated as:

$$R^* = \mu_R - \beta_{targ}^2 \mu_R^2 \delta_R^2 / (\mu_R - \mu_S) \qquad (15)$$

and the characteristic value for the normally distributed resistance is expressed as:

$$R_K = \mu_R(1 - K_R \delta_R) \qquad (16)$$

where, K_R is the parameter that determines the particular fractiles of the random variable. In the present case, 1.96 is selected in order to guarantee that at least 97.5% of the population is expected to fall above or below this fractile. By substituting Eqs. (15) & (16) into Eq. (4), the partial safety factor for the resistance can be obtained as:

$$\gamma_R = (1 - K_R \delta_R) / \left[1 - \beta_{targ}^2 \delta_R^2 / (1 - \mu_S / \mu_R)\right] \qquad (17)$$

By using the same method, γ_S can be expressed as:

$$\gamma_S = \left[1 + \beta_{targ}^2 \delta_S^2 / (\mu_R / \mu_S - 1)\right] / (1 + K_S \delta_S) \qquad (18)$$

where K_S has the same meaning as that of K_R, and the expression for S_K is:

$$S_K = \mu_S(1 + K_S \delta_S) \qquad (19)$$

As the critical design value for R and S in this study actually equals to each other, the design safety factor can be calculated as:

$$k = \gamma_R \gamma_S = R_K / S_K = \mu_R(1 - K_R \delta_R) / \mu_S(1 + K_S \delta_S) \qquad (20)$$

By subsituting μ_R into the above equation, k can be expressed in a more straigthforward format:

$$k = \frac{[\sqrt{1 - (\beta_{targ}^2 \delta_R^2 - 1)(\beta_{targ}^2 \delta_S^2 - 1)} + 1](1 - K_R \delta_R)}{(1 - \beta_{targ}^2 \delta_R^2)(1 + K_S \delta_S)} \qquad (21)$$

The relationships between the safety factors and the target

reliability index are shown in Fig.11. Compared with the results obtained for the N-LN distributions in Part 3.3, they almost exhibit the same trend. This implies that, the slight distribution difference between the load variables might not make a big difference to the calibrated safety factors when their resistance variables are both normally distributed.
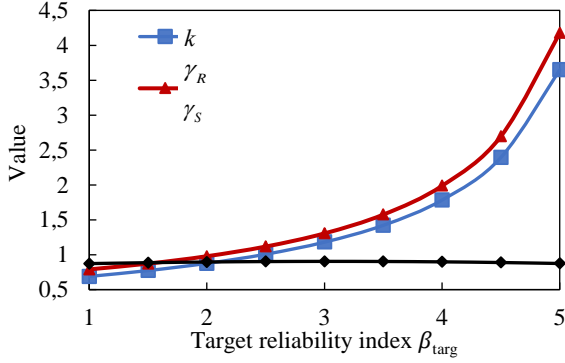

Fig.11. Safety factors vs target reliability index.

As the expressions for γ_R and γ_S are not as intuitive as that for k, and in order to have a more visual display of the variation as a function of δ_R and δ_S, the corresponding mesh plots are illustrated in Figs.12, X(a) & X(b). Note that the target reliability index is still assumed to be 4. For γ_R, it seems that δ_R does not make a big difference to its value, while for γ_S, it first shows an increasing trend when δ_S is small, and then a negative trend when δ_S reaches a certain value. With the increase of δ_S, γ_R increases while γ_S decreases most of the time. Even if γ_S is decreasing in a certain region, the design safety factor k will still remain increase as shown in Fig. 12, X(c).
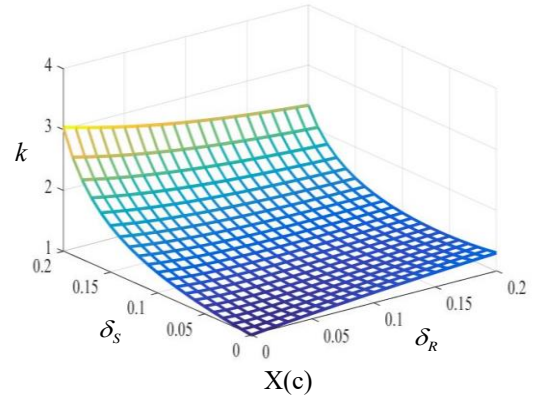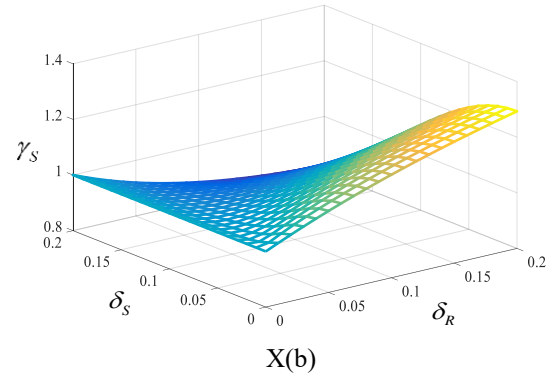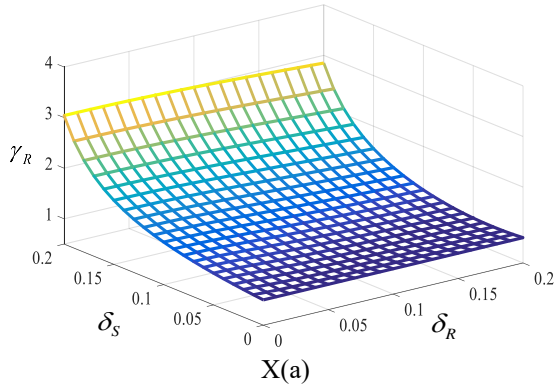

X(a)

X(b)

X(c)

Fig.12. For a given value of the reliability index equal to 4.0, X(a), X(b) and X(c) show the mesh plots of γ_R, γ_S and k vs δ_R & δ_S, respectively.

4.2. LN-LN distributions

According to manufacturing experience, the distribution type of the pipe's initial ovality is also likely to be Log-normal. By changing the statistical model of the model uncertainty while keeping the other basic variables unchanged, the distribution type for the whole resistance can also be changed. In this case, R and S are both assumed to follow Log-normal distribution.

When using the function lognrnd(*MU,SIGMA*) in Matlab to generate the random values, it should be paid attention to that, *MU* and *SIGMA* are the mean and standard deviation of the associated transformed normal variable. Therefore, with the mean value μ and coefficient of variation δ of a Log-normal distribution known, they should first be transformed using the following equations:

$$\mu_{\ln X_i} = \ln(\mu / \sqrt{1+\delta^2}) \tag{22}$$

$$\sigma_{\ln X_i} = \sqrt{\ln(1+\delta^2)} \tag{23}$$

where, the obtained $\mu_{\ln X_i}$ and $\sigma_{\ln X_i}$ are the input parameters that correspond to *MU* and *SIGMA*. As the calibration process for LN-LN distributions is also quite straightforward, some derivations can be obtained directly. With the target reliablity $\beta_{t\,arg}$ known, the logarithmic mean value of resistance $\mu_{\ln R}$ can be derived as:

$$\mu_{\ln R} = \mu_{\ln S} + \sqrt{\beta_{t\,\text{arg}}^2(\sigma_{\ln S}^2 + \sigma_{\ln R}^2)} \qquad (24)$$

where, $\mu_{\ln S}$, $\sigma_{\ln S}$ and $\sigma_{\ln R}$ can be calculated from Eqs. (22) and (23) when their corresponding mean values and coefficients of variation are given. The relationship between the design safety factor k and the target reliablity $\beta_{t\,\text{arg}}$ can be expressed as:

$$k = \exp(\sqrt{\beta_{t\,\text{arg}}^2(\sigma_{\ln S}^2 + \sigma_{\ln R}^2)} - K_R\sigma_{\ln R} - K_S\sigma_{\ln S}) \qquad (25)$$

It can be seen from Eq. (25) that, the value increases with $\beta_{t\,\text{arg}}$ in an exponential way, and this is verified by the results from the calculations which are shown in Fig.13.
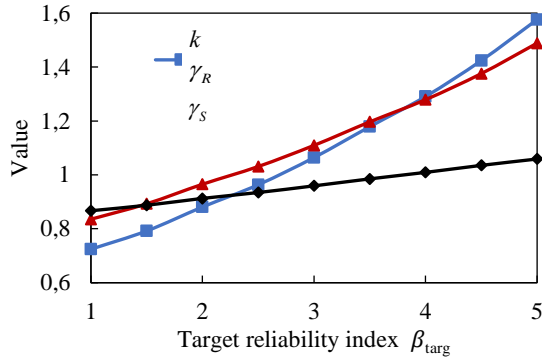
Fig.13. Safety factors vs target reliability index.

As seen from Eq. (25), $\sigma_{\ln S}$ and $\sigma_{\ln R}$, which are directly related to δ_S and δ_R, are the key factors that affect k. In turn, δ_R is closely related to the CoV of the inner radius and model uncertainty. The relationship between the design safety factor k and δ_{mod} as well as δ_{ii} are shown in Fig.14, where the target reliability index is still kept as 4. This mesh plot appears to be more like a portion from a concave surface as compared with the one in Fig.10. The larger δ_{mod} and δ_{ii} are, the larger the growth rate for the design safety factor becomes.
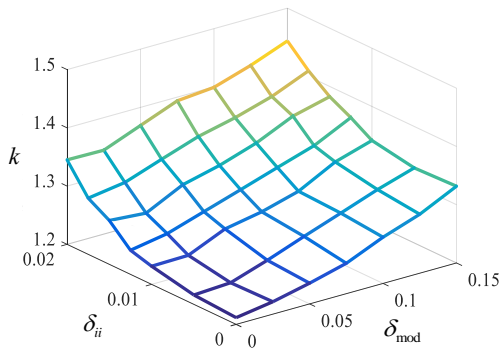
Fig.14. Design safety factor k vs δ_{mod} and δ_{ii}.

The combined effect of δ_R and δ_S are illustrated in Fig.15. When there is no uncertainty associated with both the load effect and resistance variables, the design safety factor equals 1. Generally, the design safety factor increases for increasing values of δ_R and δ_S. However, it is noted that the values at the left and right corner points

are higher than the maximum point along the diagonal. This may seem peculiar, but it should be kept in mind that the reliability index is constant throughout the considered ranges of the coefficients of variation. This artifact is accordingly due to the changing positions of the characteristic values for the resistance being different in different regions of the diagram.
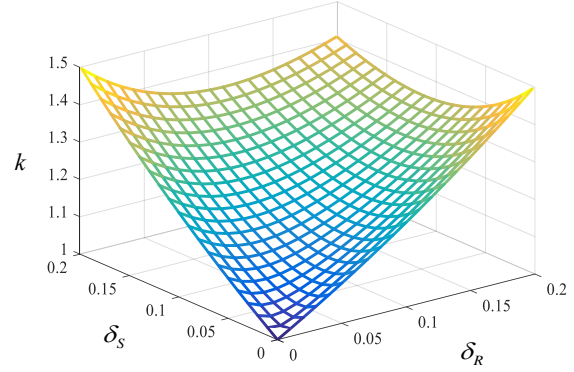

Fig.15. Design safety factor k vs δ_R and δ_S for a given value of the reliability index equal to 4.0.

4.3. LN-Gumbel distributions

The Gumbel distribution is frequently used for load effects, in particular when extreme values are considered. For the Gumbel distribution, distinction should be made between minima and maxima extreme value distributions. In our case, the maxima should be modeled, and the density function applied during the FORM calculation process is expressed as:

$$f_{X_{\max}}(x;u,\alpha) = \alpha e^{-\alpha(x-u)-e^{-\alpha(x-u)}} \qquad (26)$$

where the two distribution parameters can be obtained from the following expressions:

$$\alpha = \pi/\sqrt{6}\,\sigma \qquad (27)$$

$$u = \mu - \gamma/\alpha \qquad (28)$$

where, σ is the standard deviation of the random variable; γ is the Euler constant. The version used in Matlab is suitable for modeling minima, however, the mirror image of this distribution can be used (see Eqs. (29) and (30)) to obtain the inverse of the maxima cumulative distribution function in order to acquire its corresponding characteristic value S_K when calculating the safety factors.

$$f_{X_{\max}}(x;u,\alpha) = f_{X_{\min}}(-x;-u,1/\alpha) \qquad (29)$$

$$F_{X_{\max}}(x;u,\alpha) = 1 - F_{X_{\min}}(-x;-u,1/\alpha) \qquad (30)$$

The results in Fig.16 show that the variations of γ_R and γ_S are different from the above three cases. In this case, the curve for γ_R changes a little while the one for γ_S increases significantly, which is in contrast to the other cases. This is due to the obvious increase for both R_K and the design values when the target reliability index increases, resulting in a small change of their ratio. Anyhow, the design safety factor k is monotonously increasing as for the above three cases.
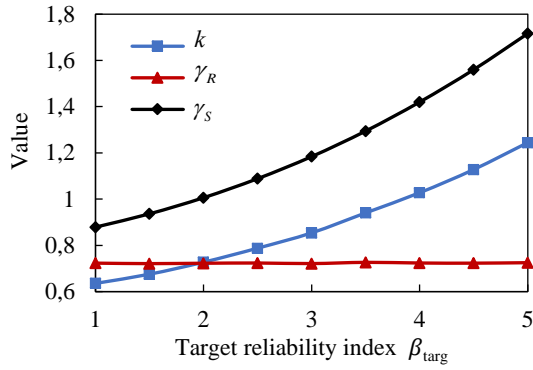
Fig.16. Safety factors vs target reliability index.

Fig.17. Comparison of design safety factor k vs target reliability index for different distribution types.

4.4. Comparison of results

Comparison between the results which are obtained by application of different distribution types are shown in Fig.17 and Fig.19. It can be observed from Fig.17 that, in the whole process, the design safety factors which correspond to the N-N distributions have the highest values, while the ones for the LN-Gumbel distributions have the lowest values. Different distribution types bring about different tendencies of the calibrated results, and this phenomenon can be explained as follows:

Suppose the probability distribution functions for the resistance and load variables are $f_R(r)$ and $f_S(s)$, respectively, and the failure probability of the pipe is expressed as:

$$P_f = \iint_{r<s} f_R(r)f_S(s)drds = \int_0^{+\infty}[1-F_S(r)]f_R(r)dr \qquad (31)$$

where $F_S(\cdot)$ is the cumulative distribution function of the load effect. Based on a geometrical interpretation of Eq. (31) which is shown in Fig.18, the failure probability of the pipe equals the enclosed area under the two curves of $1-F_S(r)$ and $f_R(r)$. The different distribution types can result in different shapes and sizes of the overlapping area for the curves which correspond to $1-F_S(r)$ and $f_R(r)$. The larger the area is, the higher the failure probability will be. Accordingly, this would be reflected in higher values of the design safety factors which are applied in order to reach the same target reliability level. Taking the N-LN and LN-LN cases as examples, the density function for normally distributed resistance has far higher values than that of the Log-normal for low resistance values (provided they have the same mean value and CoV), which results in a larger overlap area and accordingly higher values of the design safety factors. It should also be noticed that for low values of the target reliability index, the discrepancy between the design safety factors for the four different cases are not that significant. With the increase of the reliability index, the discrepancy gets more and more pronounced. This demonstrates that when the reliability level is demanding, the selection of the distribution types for both the resistance and load effect should be paid special attention to in order to obtain trustworthy and accurate results.
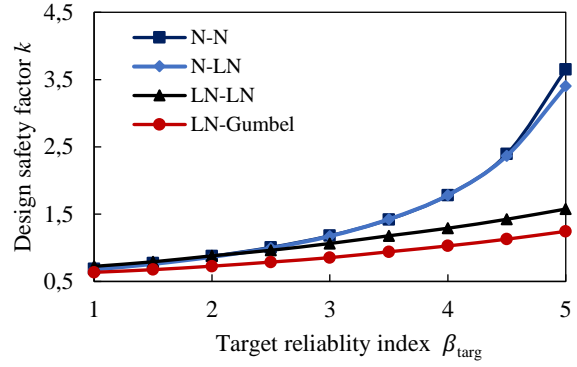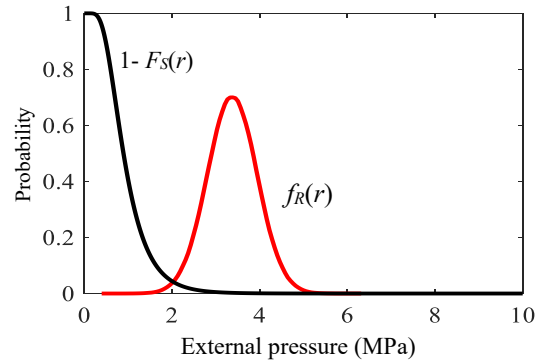

Fig.18. Geometrical expression for Eq. (31).

Fig.19 shows the design safety factor k vs reliability (i.e. 1.0 minus the failure probability) for the four cases. When the design safety factor reaches to a certain value, it will not make a big difference on the reliability of the pipe, as the failure probability of the structure reaches smaller and smaller values. With respect to practical engineering, this suggests that selecting too high values of the design safety factors lead to unnecessary conservatism.
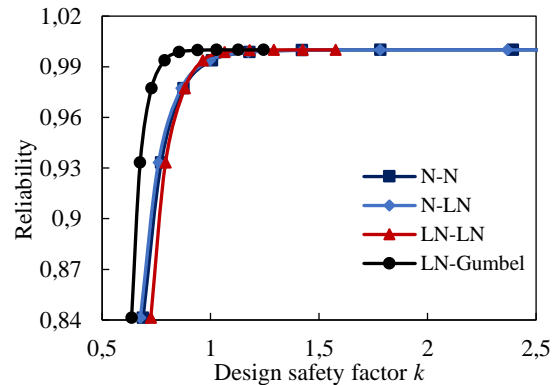

Fig.19. Design safety factor k vs reliability (i.e. 1.0 minus failure probability) for different distribution types.

5. Design Safety factor for MSFP relative to 1.5 design safety factor for metallic pipes

Even though the applied statistical models are selected based on engineering experience and design specifications, the lack of statistical data for the MSFP can still make a difference with respect to the safety factors. In the present

section, the design safety factor for the MSFP which implies the same reliability level as for metallic pipes with the widely used safety factor of 1.5 (Zhu, 1993) is considered.

Since the Log-normal distribution for the resistance and load effect are both highly recommended by the relevant specifications, the combination of LN-LN distributions is accordingly assumed at present. The load effect LN(δ_S, μ_S) applied for the metallic pipe and the MSFP are assumed to be the same, while their resistance pressures are assumed to follow different Log-normal distributions, with LN(δ_{R_0}, μ_{R_0}) for the metallic pipe and LN(δ_{R_1}, μ_{R_1}) for the MSFP. With the distribution parameters given, the reliability index for the metallic pipe in this specified working condition can be obtained from the following equation:

$$\beta = \ln\left(\frac{\mu_{R_0}}{\mu_S}\sqrt{\frac{1+\delta_S^2}{1+\delta_{R_0}^2}}\right)\bigg/\sqrt{\ln\left[(1+\delta_{R_0}^2)(1+\delta_S^2)\right]} \tag{32}$$

The target reliability index for MSFP can then be defined as the one acquired from Eq. (32) in order to reach the same reliability level. Substituting the corresponding statistical parameters and the calculated reliability index into Eq. (25), the design safety factor k_1 for the MSFP can be obtained. As the direct expression for k_1 is complicated, the design safety factor for the metallic pipe k_0 can be introduced into the expression to simplify its format and also to illustrate their relationship. As the target reliability index for metallic pipes in this specified condition is just assumed to be the corresponding calculated result from Eq. (32), the formula for k_0 can be written as:

$$k_0 = \frac{\mu_{R_0}}{\mu_S}\sqrt{\frac{1+\delta_S^2}{1+\delta_{R_0}^2}}\bigg/\exp\left\{K_f\left[\sqrt{\ln(1+\delta_{R_0}^2)}+\sqrt{\ln(1+\delta_S^2)}\right]\right\} \tag{33}$$

where, K_R and K_S are both assumed to be equal to a common value K_f for simplicity. Through formula transformation and simplification, k_1 can be expressed as:

$$k_1 = k_0\bigg/\exp\left\{\left[\ln k_0 + K_f(\sqrt{A}+\sqrt{C})\right]\left(1-\frac{\sqrt{B+C}}{\sqrt{A+C}}\right)-K_f\left[\sqrt{A}-\sqrt{B}\right]\right\} \tag{34}$$

where, A, B, C are the associated variances of the normal variables (which represent the logarithm of the lognormal variables) and are expressed as:

$$A = \ln(1+\delta_{R_0}^2) \tag{34a}$$

$$B = \ln(1+\delta_{R_1}^2) \tag{34b}$$

$$C = \ln(1+\delta_S^2) \tag{34c}$$

The coefficient of variation for resistance of metallic pipes is typically selected to be 0.03 (Jones, 1978), and for load effects the value is usually around 0.1. The relationship between the CoV of the resistance of the MSFP and the design safety factor is shown in Fig.20. The abscissa in this graph starts at the value of the CoV which equals to that of the corresponding steel material, and it can be seen that the design safety factor for the MSFP increases with δ_{R_1} in an exponential manner. For the MSFP, δ_{R_1} as calculated according to the suggested statistical model is about 0.17.

The corresponding design safety factor is then seen to be around 2. Thus, this value could be recommended as the one for MSFP's design.
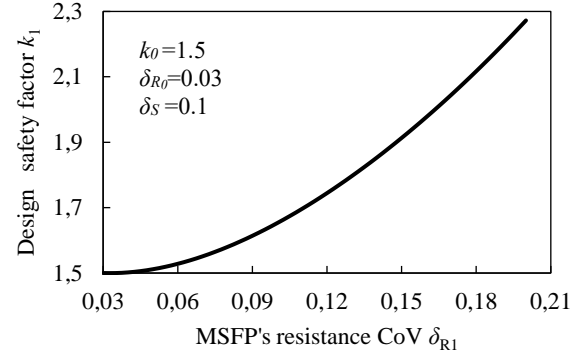

Fig.20. Design safety factor for MSFP relative to 1.5 one for metallic pipe with different CoVs for resistance.

6. Conclusions

In this paper, safety factors for metallic strip flexible pipes subjected to external pressure are calibrated, and the calibration process is illustrated in some detail. The reliability-based method which is presented serves as a useful tool in order to calibrate the safety factors for composite pipes. This applies in particular to cases where there are a large number of random variables and where iterations in relation to the mathematical model are required. The following conclusions can be drawn:

1. The design safety factors are closely related to the target reliability index and the CoV of basic variables. Generally, the design safety factors increase with the target reliability index and the CoVs of the random variables. For MSFP, the CoV of the pipe's inner radius plays a particularly important role in affecting the calibrated results, and its scatter should be controlled carefully during the manufacturing process.

2. When the reliability level is not that demanding, the distinction between the results calibrated by application of different distribution types are not that remarkable. However, when the MSFP is required to reach a high target reliability level, the distribution types of the random variables should be selected carefully in order to obtain a much more trustworthy result.

3. A design safety factor 2 is recommended to be used for design of MSFP in practical engineering. This is found to provide the same reliability level as that for conventional metallic pipes for which a design safety factor of 1.5 is widely applied.

The random variables selected in this paper might not be the optimal choice, and more data collection and more statistical analysis relating to the uncertainty modeling should be conducted. As the full statistical scatter associated with MSFP's collapse pressure has not yet been sufficiently tested to the present day, there is still a lack of verified statistical models to be applied for the purpose of calibration. If the scatter of MSFP's strength can be controlled or improved during manufacturing in the near future, the magnitude of the design safety factor

recommended above can be reduced. More suitable values can then be applied in order to avoid unnecessary conservatism.

Acknowledgement

References

Ahammed M, Melchers R E. Reliability estimation of pressurised pipelines subject to localised corrosion defects. International Journal of Pressure Vessels and Piping, 1996, 69(3): 267-272.

API RP 17B. 2008. Recommended practice for flexible pipe. American Petroleum Institute.

Avrithi K, Ayyub B M. Load and resistance factor design (LRFD) of nuclear straight pipes for loads that cause primary stress. Journal of Pressure Vessel Technology, 2010, 132(2): 021101.

Babu G L S, Srivastava A. Reliability analysis of buried flexible pipe-soil systems. Journal of pipeline systems engineering and practice, 2010, 1(1): 33-41.

Bai Q, Bai Y, Ruan W. Flexible Pipes. John Wiley & Sons, 2017.

Bai Y, Liu T, Cheng P, et al. Buckling stability of steel strip reinforced thermoplastic pipe subjected to external pressure. Journal of Composite Structures, 2016, 152: 528-537.

Bai Y, Wang N, Cheng P, et al. Collapse and Buckling Behaviors of Reinforced Thermoplastic Pipe Under External Pressure. Journal of Offshore Mechanics and Arctic Engineering, 2015, 137(4): 041401.

Bai Y, Yuan S, Cheng P, et al. Confined collapse of unbonded multi-layer pipe subjected to external pressure. Journal of Composite Structures, 2016, 158: 1-10.

Boyer C, Béakou A, Lemaire M. Design of a composite structure to achieve a specified reliability level. Journal of Reliability Engineering & System Safety, 1997, 56(3): 273-283.

dos Santos Loureiro Filho F, de Lima E C P, Sagrilo L V S, et al. Safety Factors for Fatigue Analysis of Flexible Pipes Based on Structural Reliability[C]//ASME 2012 31st International Conference on Ocean, Offshore and Arctic Engineering. American Society of Mechanical Engineers, 2012: 337-342.

Fairchild D P, Crapps J M, Cheng W, et al. Full-Scale Pipe Strain Test Quality and Safety Factor Determination for Strain-Based Engineering Critical Assessment[C]//2016 11th International Pipeline Conference. American Society of Mechanical Engineers, 2016: V002T06A003-V002T06A003.

Gibson A G, Hicks C, Wright P N H, et al. Development of glass fibre reinforced polyethylene pipes for pressure applications. Journal of plastics, rubber and composites, 2000, 29(10): 509-519.

Jones B H, Probabilistic Design and Reliability, Composite Materials, Structure Design and Analysis, Part II. Academic Press (1978).

Larin O, Barkanov E, Vodka O. Prediction of reliability of the corroded pipeline considering the randomness of corrosion damage and its stochastic growth[J]. Engineering Failure Analysis, 2016, 66: 60-71.

Leira B J, Meling T S, Larsen C M, et al. Assessment of fatigue safety factors for deep-water risers in relation to VIV. Journal of offshore mechanics and arctic engineering, 2005, 127(4): 353-358.

Leira B J, Næss A, Næss O E B. Reliability analysis of corroding pipelines by enhanced Monte Carlo simulation. International Journal of Pressure Vessels and Piping, 2016, 144: 11-17.

Leira, B.J., Baarholm, G.S., Igland, R.T., Farnes, K.A., Percy, D., 2005, "Fatigue Safety Factors for Flexible Risers based on Case Specific Reliability Analysis", 24th International Conference on Offshore Mechanics and Arctic Engineering, OMAE67432, Halkidiki, Greece, 12-17 June.

Machida H, Chitose H, Arakawa M. Partial Safety Factors Assessment of Pipes with a Circumferential Surface Flaw[C]//Proceedings of the ASME 2010 Pressure Vessels & Piping Division/KPVP Conference. 2010: 18-22.

Percy, D., 2005, "Fatigue Safety Factors for Flexible Risers based on Case Specific Reliability Analysis", 24th International Conference on Offshore Mechanics and Arctic Engineering, OMAE67432, Halkidiki, Greece, 12-17 June.

Schillo C, Kriegesmann B, Krause D. Reliability based calibration of safety factors for unstiffened cylindrical composite shells. Journal of Composite Structures, 2017, 168: 798-812.

Tee K F, Khan L R, Chen H P. Probabilistic failure analysis of underground flexible pipes. Journal of Structural Engineering and Mechanics, 2013, 47(2): 167-183.

Teixeira A P, Soares C G, Netto T A, et al. Reliability of pipelines with corrosion defects. International Journal of Pressure Vessels and Piping, 2008, 85(4): 228-237.

Veritas N. Structural reliability analysis of marine structures. Det Norske Veritas, Høvik, Norway, 1992.

Zhu T L. A reliability-based safety factor for aircraft composite structures. Journal of Computers & Structures, 1993, 48(4): 745-748.